Observation of Continuous Divertor Detachment in H-Mode Discharges in ASDEX Upgrade

O. Gruber,[1] A. Kallenbach,[1] M. Kaufmann,[1] K. Lackner,[1] V. Mertens,[1] J. Neuhauser,[1] F. Ryter,[1] H. Zohm,[1] M. Bessenrodt-Weberpals,[1] K. Büchl,[1] S. Fiedler,[2] A. Field,[1] Ch. Fuchs,[1] C. Garcia-Rosales,[1] G. Haas,[1] A. Herrmann,[1] W. Herrmann,[1] S. Hirsch,[1] W. Köppendörfer,[1] P. Lang,[1] G. Lieder,[3] K.-F. Mast,[1] C. S. Pitcher,[4] M. Schittenhelm,[1] J. Stober,[1] W. Suttrop,[1] M. Troppmann,[1] M. Weinlich,[1] M. Albrecht,[1] M. Alexander,[1] K. Asmussen,[1] M. Ballico,[1] K. Behler,[1] K. Behringer,[3] H. S. Bosch,[1] M. Brambilla,[1] A. Carlson,[1] D. Coster,[1] L. Cupido,[5] H. J. DeBlank,[1] S. De Pena Hempel,[1] S. Deschka,[1] C. Dorn,[1] R. Drube,[1] R. Dux,[1] A. Eberhagen,[1] W. Engelhardt,[1] H.-U. Fahrbach,[1] H.-U. Feist,[1] D. Fieg,[6] G. Fußmann,[1] O. Gehre,[1] J. Gernhardt,[1] P. Ignacz,[7] B. Jüttner,[1] W. Junker,[1] T. Kass,[1] K. Kiemer,[1] H. Kollotzek,[1] M. Kornherr,[1] K. Krieger,[1] B. Kurzan,[1] R. Lang,[1] M. Laux,[1] M. E. Manso,[5] M. Maraschek,[1] H.-M. Mayer,[1] P. McCarthy,[8] D. Meisel,[1] R. Merkel,[1] H. Murmann,[1] B. Napiontek,[1] D. Naujoks,[1] G. Neu,[1] R. Neu,[1] J.-M. Noterdaeme,[1] G. Pautasso,[1] W. Poschenrieder,[1] G. Raupp,[1] H. Richter,[1] T. Richter,[1] H. Röhr,[1] J. Roth,[1] N. Salmon,[1] H. Salzmann,[1] W. Sandmann,[1] H.-B. Schilling,[1] H. Schneider,[1] R. Schneider,[1] W. Schneider,[1] K. Schönmann,[1] G. Schramm,[1] U. Schumacher,[3] J. Schweinzer,[1] U. Seidel,[1] F. Serra,[5] A. Silva,[5] M. Sokoll,[1] E. Speth,[1] A. Stäbler,[1] K.-H. Steuer,[1] B. Streibl,[1] W. Treutterer,[1] M. Ulrich,[1] P. Varela,[5] H. Vernickel,[1] O. Vollmer,[1] H. Wedler,[1] U. Wenzel,[1] F. Wesner,[1] R. Wunderlich,[1] D. Zasche,[1] and H. P. Zehrfeld[1]

[1]*Max-Planck Institut für Plasmaphysik, EURATOM-IPP Association, Garching and Berlin, Germany*
[2]*Institut für Allgemeine Physik, TU Wien, Austria*
[3]*Institut für Plasmaforschung, Uni Stuttgart, Germany*
[4]*Institute for Aerospace Studies, Toronto Canada*
[5]*Centro de Fusão Nuclear, EURATOM-IST Association, Lisbon, Portugal*
[6]*Kernforschungszentrum, Karlsruhe, Germany*
[7]*Research Institute for Particle and Nuclear Physics, Budapest, Hungary*
[8]*University of Cork, Ireland*

(Received 1 December 1994)

Feedback-controlled puffing of neon and deuterium has been applied to control the edge-localized-mode behavior and the target plate power deposition during high-power H-mode discharges in ASDEX Upgrade. A regime has been found in which more than 90% of the heating power is lost through radiation and divertor detachment occurs, without deterioration of the energy confinement. The plasma remains in the H mode, exhibiting small-amplitude, high-frequency ELM's, which do not penetrate to the target plates in the strike zone region.

PACS numbers: 52.55.Fa

Reduction of the energy flux density to the target plates to below the values attainable by purely geometric spreading of the divertor fan is one of the most critical requirements for a fusion reactor [1]. Impurity radiation losses from the outer regions of the main plasma and scrape-off layer are, at present, considered the most viable option for attaining such a mode of operation [2]. The resulting state corresponds to a low-power flow to the target plates (≤ 0.1 of the total heating power), and low plasma densities and pressures in front of them, and has been termed detachment [3].

Experimentally, this aim has been pursued by raising the edge plasma density by strong gas puffing, and by the controlled introduction of light impurities. The most successful previous experiments, with strong additional heating, had involved feedback control of either the impurity puff (in TEXTOR [4]) or of the deuterium puff rate (in JET [5]). While continuous detachment could thereby be achieved in limiter and L-mode divertor discharges, experiments in H-mode resulted in either a relapse into the L regime or a reduction only of the time-averaged power flow, with heat pulses associated with edge localized modes (ELM's) still penetrating to the target plates [6,7].

The experiments on the ASDEX Upgrade reported here, were employed for the first time in a divertor tokamak feedback control of the radiated power losses through impurity (neon) addition. Simultaneously, we applied deuterium gas puffing, feedback controlling, and also the divertor neutral density. In the most successful operating mode, we attained divertor detachment both in between and during ELM's, while maintaining standard H-regime energy confinement.

Device, operating range, and diagnostics description.—ASDEX Upgrade is a midsize tokamak ($R_0 = 1.65$ m, $a = 0.5$ m, and plasma elongation $b/a = 1.6$) with a single null divertor (Fig. 1). All plasma-facing components are graphite-covered, the vessel is routinely boronized, and turbomolecular pumps allow control of the hydrogen and noble gas particle content of the vessel. The experiments described here were carried out in deuterium, with $\overline{n}_e \leq 1.2 \times 10^{20}$ m^{-3},

0031-9007/95/74(21)/4217(4)$06.00

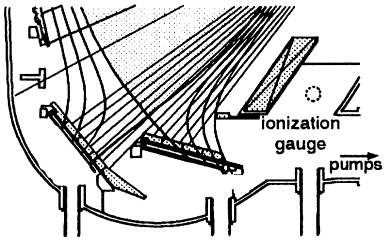

FIG. 1. Cross section of the ASDEX Upgrade divertor showing the position of ionization gauges used for the neutral flux measurements, as well as the lines of sight of the horizontal bolometer camera.

$I_p = 0.8-1.2$ MA, $|B_t| = 1.7-2.5$ T ($q_{\psi 95} = 2.7$ to 4.2), and D^0-beam injection with $P_{\mathrm{NI}} \leq 8$ MW, mainly in field orientation with the ion grad-B drift towards the target plates, favoring the H-mode access ($B_t < 0$).

The investigations reported here primarily used the following diagnostics (besides the standard set of bulk plasma diagnostics): bolometer cameras, video cameras with different filters, D_α monitors, C II and C III line emission spectroscopy, Langmuir probes in the target plates, fast target plate thermography, and ECE radiometer, reflectometry, neutral gas measurements, a lithium beam system, SX cameras, and analyzer systems for fast and slow charge exchange (CX) neutrals. Detachment was monitored, in particular, by saturation current measurements and thermography in the target plates.

Effect of gas puffing and neon addition on the H mode.—The appearance of the standard H-mode discharges is exemplified by the shot 4875, for which no neon was added, and the D_2 puff was stopped early after the onset of neutral beam (NB) heating. Such discharges reach a stationary state, with $\overline{n}_e$ in the range $(0.6-1) \times 10^{20}$ m^{-3}, and with an energy confinement corresponding to the JET/DIII-D H-mode scaling [8,9]. The divertor neutral density, monitored by the flux Γ_0^{div} into a Haas-type ionization gauge [10] at the location shown in Fig. 1, stays moderate ($\Gamma_0^{\mathrm{div}} = 10^{22}$ D_2 m^{-2} s^{-1}, corresponding to $n_{D_2}^{\mathrm{div}} \approx 3 \times 10^{19}$ m^{-3}) and the total radiated power is a fraction P_{frac}^* of 50%–60% of the heating power. The discharges exhibit type-I ELM's [11], with a frequency increasing with the applied heating power. Carbon erosion (C II line emission), thermography, and Langmuir probe measurements and video pictures taken in a C III line show clear signs of attachment during and in between ELM's.

Applying a strong deuterium puff for 2 s during the NB heating phase [7], one can significantly raise the divertor neutral density (up to 10×) and the midplane separatrix plasma density (up to 2×), but only modestly increase the average plasma density (by <30%). The D_α emission in the divertor and the radiated power fraction also rise, with P_{frac}^* reaching up to 85%. Detachment is observed in between ELM's, but the individual ELM's continue to be of large amplitude and result in transient reattachment.

With feedback-controlled neon puffing, stable H-mode discharges with $P_{\mathrm{frac}}^* > 90\%$ have been obtained. With increasing P_{frac}^*, the frequency of the type-I ELM's decreases. At a level of $P_{\mathrm{frac}}^* \approx 80\%$, long-lasting ($\approx$5 ms) "compound" ELM's [11] appear, followed by high-frequency, small ELM's (1.5 kHz compared with 160 Hz for type I) of a type III, and ELM-free periods. At a still higher radiation fraction, the compound ELM's disappear and the high-frequency ELM's form a continuous train. During this phase, the divertor plasma on the separatrix remains detached from the target plates also during the ELM's, so that a completely detached H mode (CDH) is realized.

The longest-lasting CDH phases were obtained with simultaneous feedback control of the radiation level and the divertor neutral density (No. 5028, Fig. 2). During the initial stages of the CDH phase, the central electron density and the soft x-ray emissivity slowly increase, but saturate after the appearance of the quasistationary (1, 1) mode. The electron density profiles in the CDH phase are more peaked than in a standard (type-I ELM) H mode.

After-shot deconvolution, using the full bolometer system, shows the total plasma radiation power to reach $P_{\mathrm{frac}}^* = 95\%$ (estimated errors of $\pm 5\%$), with $\approx 20\%$ originating from the scrape-off region below the X point (Fig. 2). The emission profile in the main chamber is hollow, with approximately 45% of the power radiated from either open or closed flux surfaces in a near-separatrix region, defined by the poloidal flux $\psi > 0.95\psi$ (separatrix). The concentration of neon in the central plasma remains below 1% (corresponding to a contribution $\delta Z_{\mathrm{eff}} \leq 1$), leading to a maximum of Z_{eff} of about 2.5.

The T_e and the n_e profiles obtained by ECE and lithium-beam measurements in the CDH phase still exhibit the steep H-mode gradients inside the separatrix. The energy confinement time during the CDH phase is not reduced and continues to correspond to the JET/DIII-D H-mode scaling. Referred to the ITER89 P scaling [12], the enhancement factor decreases slightly (from 1.7 for No. 4875 to 1.6 for No. 5028) due to the increased density. Typical H-mode characteristics of the CDH phase are manifested also by the signals of a nearly perpendicular looking neutral analyzer system, which has been found to see large CX fluxes from fast NBI particles only during H-mode phases (presumed to be a consequence of modifications to the ripple loss cones induced by radial E fields [13]).

Divertor detachment and ELM's.—We have studied in detail the divertor behavior during standard and CDH-phase ELM's. Figure 3 shows the results of C II line observation, Langmuir probes, and D_α emission for a corresponding pair of discharges. In the first case (No. 4875, $P_{\mathrm{frac}}^* \approx 60\%$) each ELM results in a pronounced peak in the divertor D_α emission, a high power

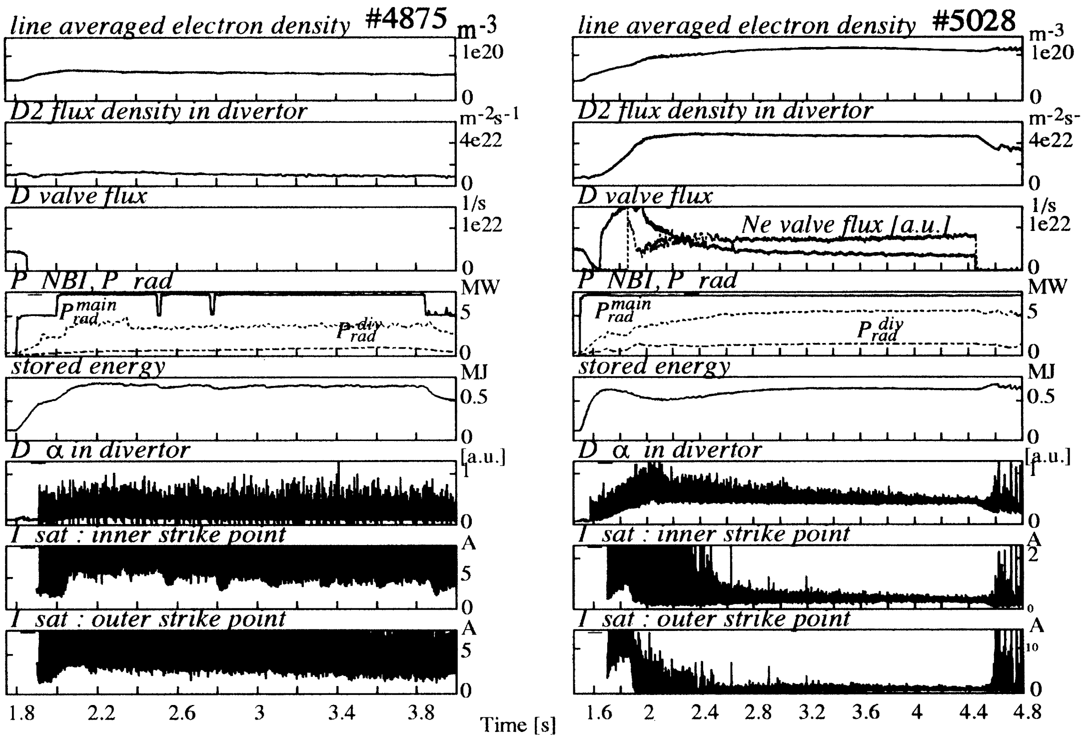

FIG. 2. Characteristic discharge parameters for a standard H-mode (4875) and for a CDH-mode discharge (5028) with neon and D_2 puffing and simultaneous feedback control of divertor neutral density and radiation power. The radiation signals give separately the radiation losses from above ($P_{\text{rad}}^{\text{main}}$) and below ($P_{\text{rad}}^{\text{div}}$) the stagnation point resulting from the after-shot analysis ($I_p = 1.0$ MA, $B_t = -2.5$ T).

pulse at the target plates, and strong C II line emission originating immediately above them. The power flow reaches peak values of >20 and time-averaged values of >3 MW/m^2. In the second case (No. 4881, $P_{\text{frac}}^* \approx 85\%$), the C II line radiation during ELM's is reduced by a factor of about 8 and originates at a distance of about 2 to 8 cm above the target plates. Video pictures (time-averaged over ELM's) taken in the C III line show the emission zone to move from the target plate (4875) to the X-point region (4881). During the CDH phase the D_α radiation is only weakly modulated by the ELM's and the time-resolved peak power flow to the target plates stays below the 1 MW/m^2 present noise limit of the fast thermography system.

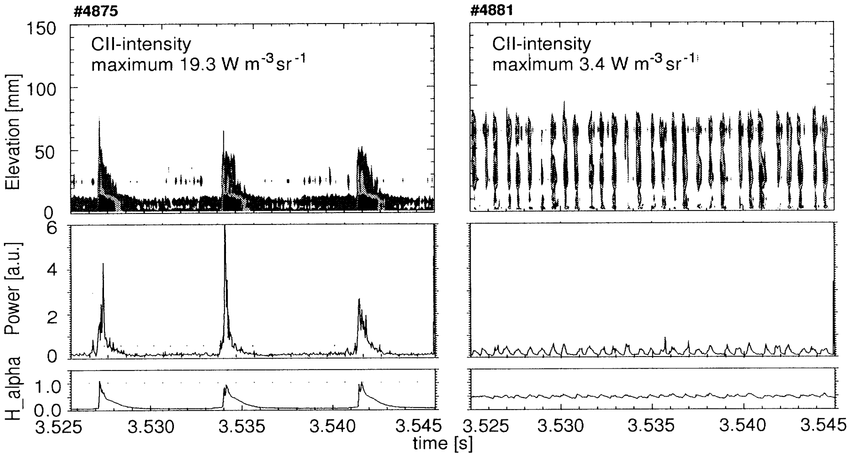

FIG. 3. Type-I ELM's (left) and ELM's during CDH phases (right). Shown is the C II line intensity as a function of the distance to target plate and time, and as a function of time, the Langmuir power flow to the target plates and D_α radiation in the divertor.

Langmuir probe measurements confirm that complete detachment at the separatrix strike point persists even during the ELM's, as is shown in Fig. 4, in a comparison between the saturation current density profiles in ELM maxima during the type-I ELM and the CDH phases of No. 4881. Detachment in between ELM's, when induced by neon puffing, occurs also nearly simultaneously at both target plates, whereas it appears clearly first only on the inside plate under other conditions.

The experiments described here have shown that the independent control of impurity radiation losses and the divertor neutral density can significantly broaden the operating space of tokamaks in the critical parameter combination of energy confinement time and peak target plate heat load. Simultaneous feedback control on deuterium and neon gas puffs gives access to conditions with good H-mode plasma confinement and negligible peak and time-averaged power fluxes to the target plates. This CDH regime is characterized by small, high-frequency type-III ELM's which do not lead to reattachment in the separatrix strike-point region.

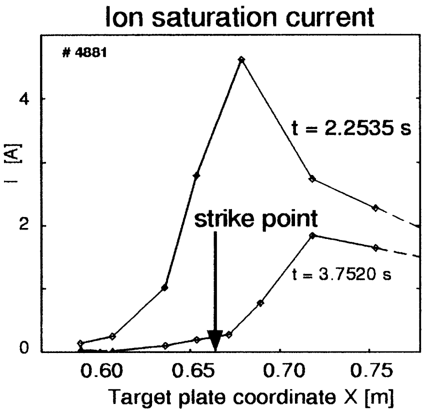

FIG. 4. Ion saturation current profile on the outer target plate during the ELM peaks, in the type-I ELM and the CDH phases of a discharge.

---

[1] ITER Central Team, Plasma Phys. Controlled Fusion 35 Suppl. (**12**), B23 (1993).
[2] K. Lackner and R. Schneider, Fus. Eng. Design **22**, 107 (1993).
[3] P.C. Stangeby, Nucl. Fusion **33**, 1695 (1993).
[4] U. Samm *et al.,* J. Nuclear Mater. **196–198**, 633 (1992).
[5] G. Janeschitz *et al.,* Proceedings of 19th European Conference on Controlled Fusion and Plasma Physics, Innsbruck, 1992 (unpublished), Vol. II, p. 727.
[6] T.W. Petrie, A.G. Kellman, and M. Ali Mahdavi, Nucl. Fusion **33**, 929 (1993).
[7] K. Lackner *et al.,* Plasma Phys. Controlled Fusion (to be published).
[8] F. Ryter *et al.,* Plasma Phys. Controlled Fusion 36 Suppl. **7**, A99 (1994).
[9] D.P. Schissel *et al.,* Nucl. Fusion **31**, 73 (1991).
[10] G. Haas *et al.,* J. Nucl. Mater. **121**, 151 (1984).
[11] H. Zohm *et al.,* Nucl. Fusion (to be published).
[12] P.N. Yushmanov *et al.,* Nucl. Fusion **30**, 1999 (1990).
[13] A. Herrmann (to be published).